Published in final edited form as:
J Heart Lung Transplant. 2010 January ; 29(1): 13. doi:10.1016/j.healun.2009.05.034.

AN INNOVATIVE, SENSORLESS, PULSATILE, CONTINUOUS-FLOW TOTAL ARTIFICIAL HEART: DEVICE DESIGN AND INITIAL *IN VITRO* STUDY

Kiyotaka Fukamachi, MD, PhD, **David J. Horvath, MSME**, **Alex L. Massiello, MEBME**, **Hideyuki Fumoto, MD**, **Tetsuya Horai, MD**, **Santosh Rao, MD**, and **Leonard A. R. Golding, MB, BS, FRACS**
Department of Biomedical Engineering, Lerner Research Institute, Cleveland Clinic 9500 Euclid Avenue, Cleveland, OH 44195

Abstract

Background—We are developing a very small, innovative, continuous-flow total artificial heart (CFTAH) that passively self-balances left and right pump flows and atrial pressures without sensors. This report details the CFTAH design concept and our initial *in vitro* data.

Methods—System performance of the CFTAH was evaluated using a mock circulatory loop to determine the range of systemic and pulmonary vascular resistances (SVR and PVR) over which the design goal of a maximum absolute atrial pressure difference of 10 mm Hg is achieved for a steady-state flow condition. Pump speed was then modulated at 2,600 ± 900 rpm to induce flow and arterial pressure pulsation to evaluate the effects of speed pulsations on the system performance. An automatic control mode was also evaluated.

Results—Using only passive self-regulation, pump flows were balanced and absolute atrial pressure differences were maintained below 10 mm Hg over a range of SVR (750-2,750 dyne·sec·cm^{-5}) and PVR (135-600 dyne·sec·cm^{-5}) values far exceeding normal levels. The magnitude of induced speed pulsatility affected relative left/right performance, allowing for an additional active control to improve balanced flow and pressure. The automatic control mode adjusted pump speed to achieve targeted pump flows based on sensorless calculations of SVR and CFTAH flow.

Conclusions—The initial *in vitro* testing of the CFTAH with a single, valveless, continuous-flow pump demonstrated its passive self-regulation of flows and atrial pressures and a new automatic control mode.

The clinical use of left ventricular assist devices (LVADs) is becoming more widely accepted, due in large part to the introduction of continuous-flow blood pumps.1-6 These newer devices show significant improvements in size, simplicity, reliability, durability, and clinical results. However, 20-50% of patients undergoing LVAD implantation also have significant right ventricular failure, which limits the utility of implantable LVAD therapy.7-11 Existing total artificial hearts (TAHs) are either a temporary pneumatic system (CardioWest™, SynCardia, Tucson, AZ) with an externalized pneumatic driver or a permanent pulsatile implantable

Corresponding Author: Leonard A. R. Golding, MB, BS, FRACS Department of Biomedical Engineering / ND20 Cleveland Clinic, 9500 Euclid Avenue, Cleveland, OH 44195 Phone: (216) 444-1205; Fax: (216) 444-9198: E-mail: goldinl@ccf.org.

system (AbioCor™, Abiomed®, Danvers, MA). To date, they have demonstrated significant limitations in initial clinical trials because of their large size, limited durability, and incidence of thrombus formation and embolization.[12] The inherent design characteristics of these pulsatile systems prevent significant reductions in size.

The feasibility of native heart replacement with two separate continuous-flow pumps has recently been demonstrated at the Texas Heart Institute (Houston, TX)13 and Tohoku University (Sendai, Japan).14 These systems require duplication of pump components, increasing the potential for component failure and necessitating the development of complex algorithms to appropriately coordinate the outputs of the two pumps. We are developing a continuous-flow TAH (CFTAH) that is extremely innovative, exploring radical new concepts in TAH design. The proposed concept involves the use of a valveless, sensorless, continuous-flow pump and automatic control system. This double-pump concept comprises a single, continuously rotating, brushless DC motor and a pump assembly with a centrifugal pump on both ends. Pump speed will be modulated to create pulsatile flow and pressure. This report details the CFTAH design concept and our initial *in vitro* data in a mock circulatory loop.

Methods

Design of the Baseline Blood Pump

The CFTAH replaces both ventricles of the heart and delivers blood flow to both the systemic and pulmonary circulations from a single pump assembly (Figure 1). This device has one motor and one rotating assembly (rotor) supported on a hydrodynamic bearing. Impellers supporting the left and right circulations are mounted on opposing ends of the rotor, allowing the left and right hydraulic environments to create opposing forces at opposite ends of the rotor. Features of a pressure regulator are integrated into the pumping element design to passively self-balance left and right flows and atrial pressures.

Design Requirements of CFTAH

The following design requirements are used to serve as a target for the baseline design: (1) systemic flow of 3-8 L/min, (2) systemic vascular resistance (SVR) of 700-2,000 dyne·sec·cm^{-5}, (3) pulmonary vascular resistance (PVR) of 100-500 dyne·sec·cm^{-5}, (4) maximum atrial pressure difference of 10 mm Hg., (5) minimum right and left atrial pressures (RAP and LAP) of 0 mm Hg at extreme vascular resistances, and (6) maximum RAP and LAP of 20 mm Hg at extreme vascular resistances.

Passive Self-Regulation of Left/Right Flow and Atrial Pressure Balance

The motor's magnet assembly is embedded in the rotating assembly, and it is shorter than the motor's steel laminations, allowing a degree of free axial movement, primarily caused by a pump inlet (atrial) pressure difference (Figure 2). This axial movement changes the area of the aperture at the outer diameter (OD) of the right impeller, affecting relative left/right performance in a direction to correct the atrial pressure imbalance as described below.

The key to our CFTAH passive self-regulating design is based on three direct relationships: 1) the axial position of the rotor has a direct relationship to the pump inlet (atrial) pressure difference, 2) there is a direct relationship between the axial position of the rotor and the size of the right pump aperture, and 3) there is a direct relationship between the aperture size and the hydraulic output of the right pump. If there is a physiologic change that causes the left pump to produce less flow than the right pump, the LAP will rise rapidly, pushing the rotor to the right, thereby reducing the right pump aperture size and reducing the right output to reduce LAP. If the left pump is producing more flow than the right, the RAP rises, pushing the rotor to the left, opening the aperture of the right pump, increasing the right output to reduce RAP.

Meanwhile, the corresponding changes in clearances around the left impeller cause a relatively smaller effect on left pump hydraulic output for all rotor positions. Thus, rotor axial position effects on CFTAH passive self-regulation are primarily right side effects.

Active Speed Modulation for Additional Means of Maintaining Left/Right Balance

Speed modulation can be used as a potential additional means of maintaining the left/right balance. Because the controlling aperture is at the OD of the right impeller, a modulated speed will create a corresponding pulsatile buildup of pressure within the right inlet, causing the rotor position to vary with the cycling speed amplitude. As described above, when the rotor is at the left position, the right pump aperture is open at all times and right output is maximized. If the speed is then cycled, the rotor cycles from the left to right position and the aperture cyclically opens and closes, decreasing the net right pump output. When the rotor is at the right position, the right pump aperture is reduced at all times and right output is decreased. If the speed is then cycled, the rotor cycles from the right to left position and the aperture cyclically opens, increasing the net right pump output. Because of this, speed modulation effects on flow and pressure balance are also predominantly on the right side.

Automatic Control of Speed

An automatic control mode has been implemented to raise or lower the mean pump speed to achieve a target flow depending on the calculated SVR. Both systemic output (left pump flow) and SVR are closely correlated with functions of motor power and speed, providing the basis for this control algorithm of target systemic flow vs. SVR. Figure 3 shows an example of a programmed target systemic flow vs. SVR relationship. It is anticipated that target flow should decrease with high SVR so that a high systemic arterial pressure is not enforced by the pump and target flows should increase with vasodilation. The end points (maximum and minimum target flow) define the slope or responsiveness of this control relationship and can be optimized to individual patient size and physiologic needs by physicians.

Figure 4 demonstrates the close correlations between functions of motor power and speed and both systemic output and SVR. These close correlations are independent of PVR, pump speed and speed modulation, and level of pump output, as these data cover a range in PVR of 130-600 dyne·sec·cm^{-5}, average pump speeds of 2,500 and 3,000 rpm, operation in both constant speed and at a sinusoidal modulated speed waveform of up to ±25% of the average speed, and flows between 3.2 and 7 L/min. From these linear relationships, SVR and the left pump flow are calculated in the system's control module. No flow, pressure, or other sensors are needed to estimate SVR and flow. These relationships allow for reliable implementation of the proposed CFTAH automatic control. Based on the active speed modulation data discussed below, also implemented in this control algorithm was a decrease in the amplitude of speed modulation for high conditions of SVR.

In Vitro System Performance Test Methods

The CFTAH system performance described above was evaluated using the CFTAH mock circulatory loop (Figure 5). Solid lines show the standard loop with normal simulated systemic and pulmonary circulations; dashed lines show the *alternative* fluid paths when left and right pump performance was tested independently (the left pump pumped to the left reservoir and the right pump to the right reservoir). A mixture of water and glycerin (specific gravity 1.060) was used as working fluid.

Passive Self-Regulation Test—To demonstrate the effect of rotor position on individual left and right pump performance, *in vitro* performance data for both pumps were obtained using the alternative loop configuration at a pump speed of 2,600 rpm. Individual pump flows were plotted at various differential pressures to compare the pump performance for the rotor position

to the right (LAP - RAP of 10 mm Hg) and for the rotor position to the left (LAP - RAP of -10 mm Hg).

Active Speed Modulation Test—To evaluate the effects of speed modulation on the left and right pump performance, sinusoid speed pulsatility (2,600 ± 900 rpm) was added at 80 bpm to the same conditions as described in passive self-regulation test using the alternative loop.

Extreme Variation and Mismatches of SVR and PVR—Overall system range of operation combining passive self-regulation and active speed modulation was evaluated using the standard loop. Performance mapping was extended beyond normal physiologic conditions to extreme variation and mismatches of SVR and PVR. Data were taken at fixed mean speeds of 2,500 and 3,000 rpm, with flows ranging from 3.2 to 7.0 L/min and the degree of speed modulation (0 to ± 25% of mean speed) based on calculated SVR. SVR and PVR were varied (SVR: 750-2,750 dyne·sec·cm^{-5} and PVR: 135-600 dyne·sec·cm^{-5}) to obtain atrial pressure differences (LAP-RAP) of -5, 0, and 7 mm Hg, which fall within our CFTAH system requirement of a maximum ±10 mm Hg atrial pressure difference.

Automatic Control Test—The CFTAH was operated in automatic control mode in the standard loop while SVR was varied between 600 and 2,200 dyne·sec·cm^{-5}. In this test, the targeted systemic flow was derived based on the SVR relationship shown in Figure 3. The measured left pump flow vs. measured SVR relationship was compared with targeted left pump flow vs. calculated SVR relationship to demonstrate the accuracy of the automatic control mode.

Results

Passive Self-Regulation

Figure 6 demonstrates the performance of the left and right pumps with rotor position to the left (LAP - RAP of -10 mm Hg) and rotor position to the right (LAP - RAP of 10 mm Hg). The left pump performance curves are almost identical at these two conditions, demonstrating minimal effects of the rotor position on the left pump performance. The right pump output increases markedly with the rotor position to the left compared with the rotor position to the right. This demonstrates increased right pump performance when the RAP is much higher than the LAP, resulting in a self-regulating system. The net effect of the differential atrial pressure balance on the rotor position, the left and right pump hydraulic performance, and atrial pressures are tabulated in Table 1. These data demonstrate that most of the self-regulation is in the right pump and is in response to variation in the difference between left and right pump inlet pressure (LAP-RAP).

Active Speed Modulation

Figure 7 demonstrates the flow performance of the left and right pumps with and without speed modulation while the rotor position is to the left (LAP - RAP of -10 mm Hg). Both left and right pump performance curves decreased slightly with speed modulation. Figure 8 demonstrates the effect of speed modulation on flow performance of the left and right pumps with the rotor position to the right (LAP - RAP of 10 mm Hg). Although left pump performance curve slightly decreased similar to the data in Figure 7, the right pump performance curves show a markedly increased output with speed modulation. Therefore, modulation of speed pulsatility can be used to significantly affect left and right flow and pressure balance when the rotor position is to the right or when LAP is significantly higher than RAP.

Extreme Variation and Mismatches of SVR and PVR

Figure 9 demonstrates the resulting overall system range of operation with extreme variation and mismatches of SVR and PVR. The two lines labeled with note 1 are at an (LAP-RAP) of -5 mm Hg and a speed modulation of ±25%. The lines labeled with note 2 are for (LAP-RAP) of 0 mm Hg and a speed modulation of ±25%. The lines labeled with note 3 at high SVR conditions are at an (LAP-RAP) of 10 mm Hg, and speed modulation decreased to zero as per the theory of active speed modulation above. Note that the demonstrated range of stable self-regulation greatly exceeds the plotted box showing the normal range of SVR and PVR.

Automatic Control of Speed

Figure 10 compares the actual measured left pump flow vs. measured SVR relationship with the derived target left pump flow vs. calculated SVR relationship while operating in automatic control mode under the programmed flow / SVR relationship shown in Figure 3. The controller actively adjusted pump speed and speed modulation to match measured pump flow to the derived target flows in response to calculated SVR values, demonstrating the automatic control capabilities.

Discussion

Our novel concept has been developed based on our prior efforts in successfully designing the CorAide™ continuous-flow LVAD using a noncontacting blood journal bearing and sensorless automatic control.[15,16] We have also drawn on 20 years of experience in pulsatile TAH design incorporating basic design requirements for providing systemic flows, implantability, and inherent passive balancing of the left and right flows.[17-35] The CFTAH design, however, is extremely innovative, exploring radical new concepts in TAH design in the use of a speed modulated, single shaft, dual centrifugal pump without the use of valves and sensors for control, which greatly decreases the pump size and improves system reliability.

Due to the relatively high number of complex components that comprise existing TAHs and biventricular assist devices, their potential for failure, large size, and limited duration of use all create an obvious need for a small, reliable TAH that can be implanted in any patient, regardless of size. The availability of a small, simplified alternative that has a single moving component would address many of the problems with existing technologies and provide better management for many patients who presently have no treatment option except transplantation. Ultimately, such a device would be less costly due to the need for only a single motor controller to balance left and right flows, while eliminating valves, compliance chambers, actuator mechanisms, and sensors. The relative simplicity of the CFTAH design is indicated in Table 2.

Lack of preload sensitivity has always been one of the leading factors preventing use of continuous-flow devices for LVAD or TAH applications. Equally revolutionary is our proposed control scheme to use passive self-balancing of pump flows to maintain flow/atrial pressure balance. A balanced flow and atrial pressure state is defined here by stable pump flows and stable (yet not necessarily equal) atrial pressures. Any transient imbalance in flows as a result of changing vascular resistances is automatically accompanied by a change in the atrial pressure balance that is used as the passive hydraulic pressure feedback, allowing passive autoregulation of relative left and right pump performance to return the system to a balanced flow and pressure state.

The CFTAH self-regulating response also acts to reverse atrial suction. For example, if the left inlet is occluded due to suction of tissue around the inlet, the left inlet pressure will drop, pulling

the rotor to the left, thereby maximizing the hydraulic output of the right pump, increasing pulmonary flow and LAP and thus automatically recovering from the suction condition.

Examination of the condition of high SVR (2200-2800 dyne·sec·cm-5) in dataset 3 of Figure 9 provides an example of the system's combined passive and active regulation of flows and pressures. In response to increased SVR, the left pump flow decreases relative to the right, and LAP increases relative to RAP. The resulting increase in LAP/RAP pressure differential caused the CFTAH rotor to move to the right, closing the right pump aperture, decreasing its hydraulic performance relative to the left pump. This passive autoregulation was augmented by the automatic speed control action to decrease the speed modulation to a nonpulsatile state in response to high calculated SVR, further decreasing right pump output relative to the left pump and limiting LAP-RAP mismatch to only +7 mm Hg.

Acute *in vivo* experiments are under way to validate *in vivo* pump performance with the current CFTAH design. The CFTAH will be further improved and refined and be subjected to further chronic *in vivo* pump performance, biocompatibility, and reliability in preclinical studies.

Conclusions

The initial *in vitro* testing of the innovative CFTAH with a single, valveless, continuous-flow pump successfully demonstrated passive autoregulation of left-right flow and atrial pressure balance without the need for sensors. Accurate estimation of pump flow and SVR enabled us to implement the automatic control algorithm.

Acknowledgments

Acknowledgements, funding and disclosures of conflicts for all authors This study was supported by the Trawick Fund and by grant 1R21HL089052 (P.I.: L. Golding), awarded by the National Heart, Lung, and Blood Institute, National Institutes of Health. None of the authors have a financial interest or other potential conflict of interest related to subject matter or materials mentioned in the manuscript.

Sources of Funding: This study was supported by the Trawick Fund and by grant 1R21HL089052 (P.I.: L. Golding), awarded by the National Heart, Lung, and Blood Institute, National Institutes of Health.

References

1. Miller LW, Pagani FD, Russell SD, et al. Use of a continuous-flow device in patients awaiting heart transplantation. N Engl J Med 2007;357:885–96. [PubMed: 17761592]
2. Wilhelm MJ, Hammel D, Schmid C, et al. Long-term support of 9 patients with the DeBakey VAD for more than 200 days. J Thorac Cardiovasc Surg 2005;130:1122–9. [PubMed: 16214529]
3. Haj-Yahia S, Birks EJ, Rogers P, et al. Midterm experience with the Jarvik 2000 axial flow left ventricular assist device. J Thorac Cardiovasc Surg 2007;134:199–203. [PubMed: 17599509]
4. Esmore D, Kaye D, Spratt P, et al. A prospective, multicenter trial of the VentrAssist left ventricular assist device for bridge to transplant: safety and efficacy. J Heart Lung Transplant 2008;27:579–88. [PubMed: 18503955]
5. Morshuis M, El-Banayosy A, Arusoglu L, et al. European experience of DuraHeart magnetically levitated centrifugal left ventricular assist system. Eur J Cardiothorac Surg. Feb 20;2009 Epub ahead of print.
6. Wood C, Maiorana A, Larbalestier R, Lovett M, Green G, O'Driscoll G. First successful bridge to myocardial recovery with a HeartWare HVAD. J Heart Lung Transplant 2008;27:695–7. [PubMed: 18503974]
7. Fukamachi K, McCarthy PM, Smedira NG, Vargo RL, Starling RC, Young JB. Preoperative risk factors for right ventricular failure after implantable left ventricular assist device insertion. Ann Thorac Surg 1999;68:2181–4. [PubMed: 10616999]

8. Ochiai Y, McCarthy PM, Smedira NG, et al. Predictors of severe right ventricular failure after implantable left ventricular assist device insertion: analysis of 245 patients. Circulation 2002;106(12 Suppl 1):I198–202. [PubMed: 12354733]
9. Dang NC, Topkara VK, Mercando M, et al. Right heart failure after left ventricular assist device implantation in patients with chronic congestive heart failure. J Heart Lung Transplant 2006;25:1–6. [PubMed: 16399523]
10. Matthews JC, Koelling TM, Pagani FD, Aaronson KD. The right ventricular failure risk score a preoperative tool for assessing the risk of right ventricular failure in left ventricular assist device candidates. J Am Coll Cardiol 2008;51:2163–72. [PubMed: 18510965]
11. Potapov EV, Stepanenko A, Dandel M, et al. Tricuspid incompetence and geometry of the right ventricle as predictors of right ventricular function after implantation of a left ventricular assist device. J Heart Lung Transplant 2008;27:1275–81. [PubMed: 19059106]
12. Dowling RD, Gray LA Jr. Etoch SW, et al. Initial experience with the AbioCor implantable replacement heart system. J Thorac Cardiovasc Surg 2004;127:131–41. [PubMed: 14752423]
13. Frazier OH, Tuzun E, Cohn WE, Conger JL, Kadipasaoglu KA. Total heart replacement using dual intracorporeal continuous-flow pumps in a chronic bovine model: a feasibility study. ASAIO J 2006;52:145–9. [PubMed: 16557099]
14. Olegario PS, Yoshizawa M, Tanaka A, et al. Outflow control for avoiding atrial suction in a continuous flow total artificial heart. Artif Organs 2003;27:92–8. [PubMed: 12534719]
15. Fukamachi K, Ochiai Y, Doi K, et al. Chronic evaluation of the Cleveland Clinic CorAide left ventricular assist system in calves. Artif Organs 2002;26:529–33. [PubMed: 12072109]
16. Doi K, Golding LA, Massiello AL, et al. Preclinical readiness testing of the Arrow International CorAide left ventricular assist system. Ann Thorac Surg 2004;77:2103–10. [PubMed: 15172276]
17. Irie H, Harasaki H, Massiello A, et al. Anatomic study for in vivo evaluation of a total artificial heart in calves. ASAIO Trans 1991;37:M219–20. [PubMed: 1751118]
18. Fukamachi K, Irie H, Massiello A, et al. Effects of mechanical ventilation and spontaneous respiration on hemodynamics in calves with total artificial hearts. ASAIO J 1992;38:M493–6. [PubMed: 1457909]
19. Irie H, Massiello A, Kiraly R, et al. Initial in vivo tests of an electrohydraulic actuated total artificial heart. ASAIO J 1992;38:M497–500. [PubMed: 1457910]
20. Fukamachi K, Fukumura F, Kiraly RJ, et al. Hemodynamic changes with posture in calves with total artificial heart. ASAIO J 1993;39:M419–22. [PubMed: 8268570]
21. Fukamachi K, Massiello AL, Kiraly RJ, et al. Effects of a total artificial heart right stroke volume limiter on left-right hemodynamic balance. ASAIO J 1993;39:M410–4. [PubMed: 8268568]
22. Rintoul TC, Butler KC, Thomas DC, et al. Continuing development of the Cleveland Clinic-Nimbus total artificial heart. ASAIO J 1993;39:M168–71. [PubMed: 8268522]
23. Harasaki H, Fukamachi K, Massiello A, et al. Progress in Cleveland Clinic-Nimbus total artificial heart development. ASAIO J 1994;40:M494–8. [PubMed: 8555565]
24. McCarthy PM, Fukamachi K, Fukumura F, Muramoto K, Golding LA, Harasaki H. The Cleveland Clinic-Nimbus total artificial heart. In vivo hemodynamic performance in calves and preclinical studies. J Thorac Cardiovasc Surg 1994;108:420–8. [PubMed: 8078335]
25. Fukamachi K, Benavides ME, Wika KE, Manos JA, Massiello AL, Harasaki H. Assessment of circulating blood volume in calves with a total artificial heart. ASAIO J 1995;41:M262–5. [PubMed: 8573802]
26. Harasaki H, Fukamachi K, Benavides M, Manos J, Wika K, Massiello A. A comprehensive hematologic study in calves with total artificial hearts. ASAIO J 1995;41:M266–71. [PubMed: 8573803]
27. Fukamachi K, Harasaki H, Massiello AL, Chen JF, Kiraly RJ. In vitro evaluation of automatic control performance of a total artificial heart with changes in pump orientation. ASAIO J 1996;42:M589–92. [PubMed: 8944949]
28. Fukamachi K, McCarthy PM, Vargo R, et al. Anatomic fitting studies of a total artificial heart in heart transplant recipients. Critical dimensions and prediction of fit. ASAIO J 1996;42:M337–42. [PubMed: 8944902]

29. Doi K, Smith WA, Harasaki H, et al. In vivo studies of the MagScrew total artificial heart in calves. ASAIO J 2002;48:222–5. [PubMed: 12058993]

30. Weber S, Doi K, Massiello AL, et al. In vitro controllability of the MagScrew total artificial heart system. ASAIO J 2002;48:606–11. [PubMed: 12455770]

31. Schenk S, Weber S, Luangphakdy V, et al. MagScrew total artificial heart in vivo performance above 200 beats per minute. Ann Thorac Surg 2005;79:1378–83. discussion 1383. [PubMed: 15797082]

32. Weber S, Kamohara K, Klatte RS, et al. MagScrew TAH: an update. ASAIO J 2005;51:xxxvi–xlvi. [PubMed: 16340348]

33. Kamohara K, Weber S, Klatte RS, et al. Replacement of the left-side valves of an implanted total artificial heart. ASAIO J 2006;52:368–72. [PubMed: 16883114]

34. Schenk S, Weber S, Smith WA, Fukamachi K. MagScrew total artificial heart. Ann Thorac Surg 2006;81:2338–9. [PubMed: 16731199]

35. Kamohara K, Weber S, Klatte RS, et al. Hemodynamic and metabolic changes during exercise in calves with total artificial hearts of different sizes yet similar output. Artif Organs 2007;31:667–76. [PubMed: 17725694]

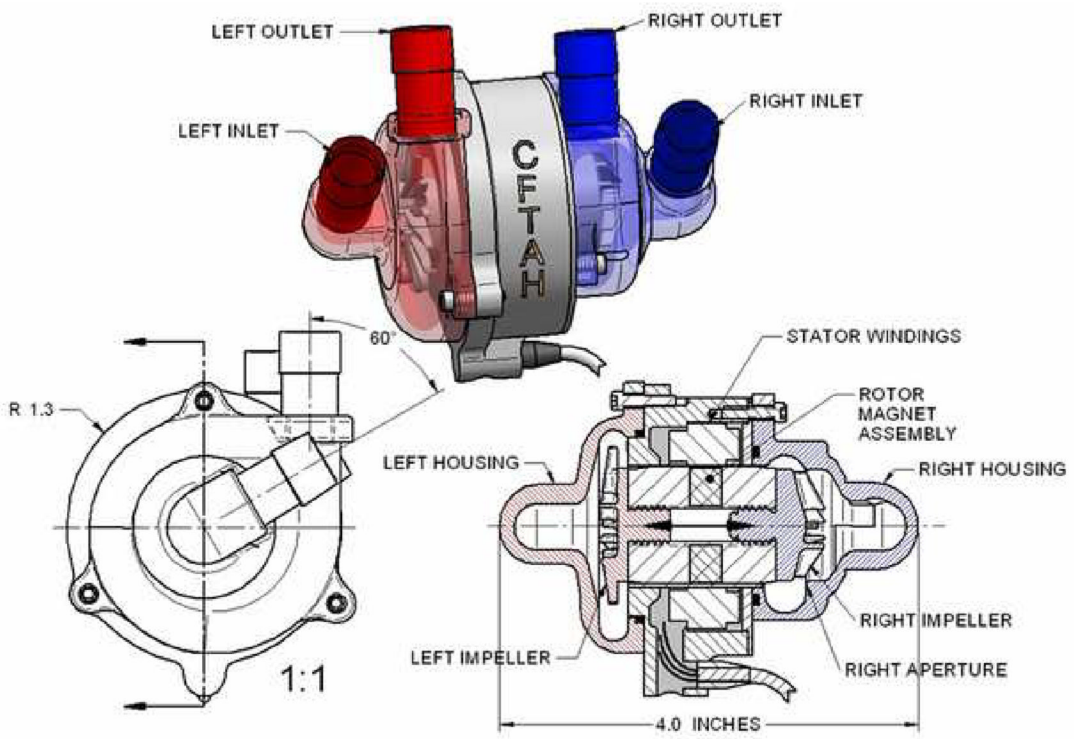

Figure 1.
Continuous-flow total artificial heart (CFTAH) pump configuration.

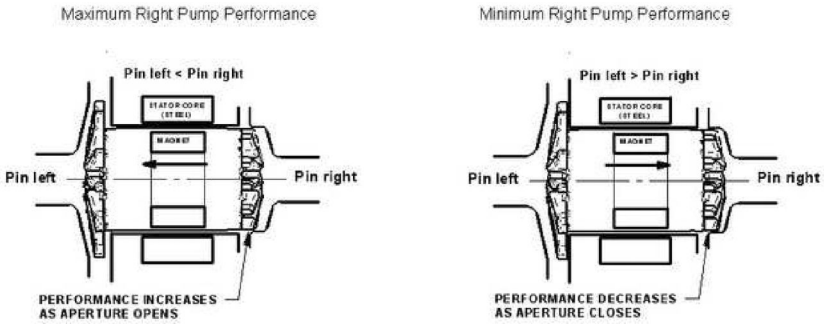

Figure 2.
Atrial pressure differential effects on rotor position and right pump performance.

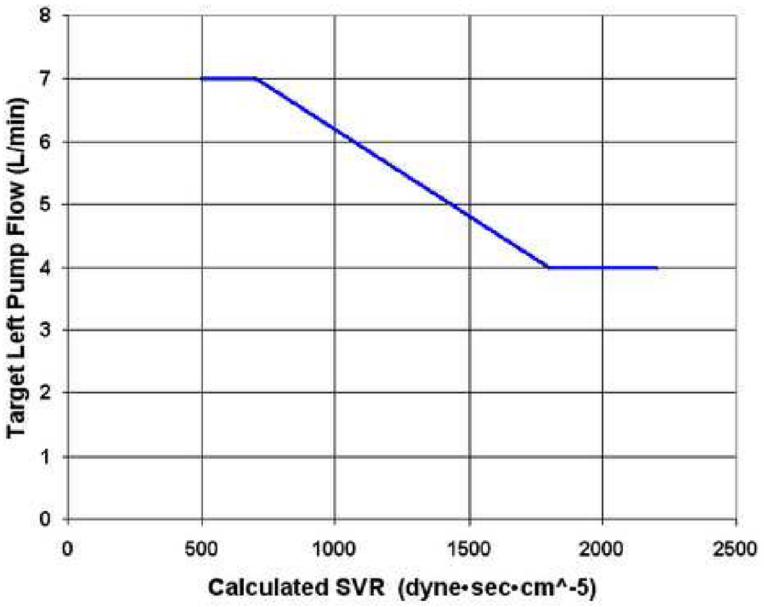

Figure 3.
Example of physician prescribed schedule of target flow vs. SVR. SVR, systemic vascular resistance.

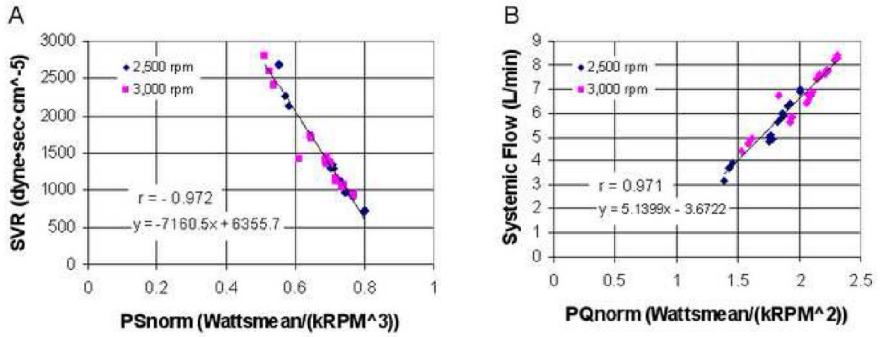

Figure 4.

(A) Systemic vascular resistance and (B) CFTAH flow correlation with motor power and speed. SVR, systemic vascular resistance; PSnorm = [mean motor power (W)] / [mean pump speed (krpm)^3]; PQnorm = [mean motor power (W)] / [mean pump speed (krpm)^2].

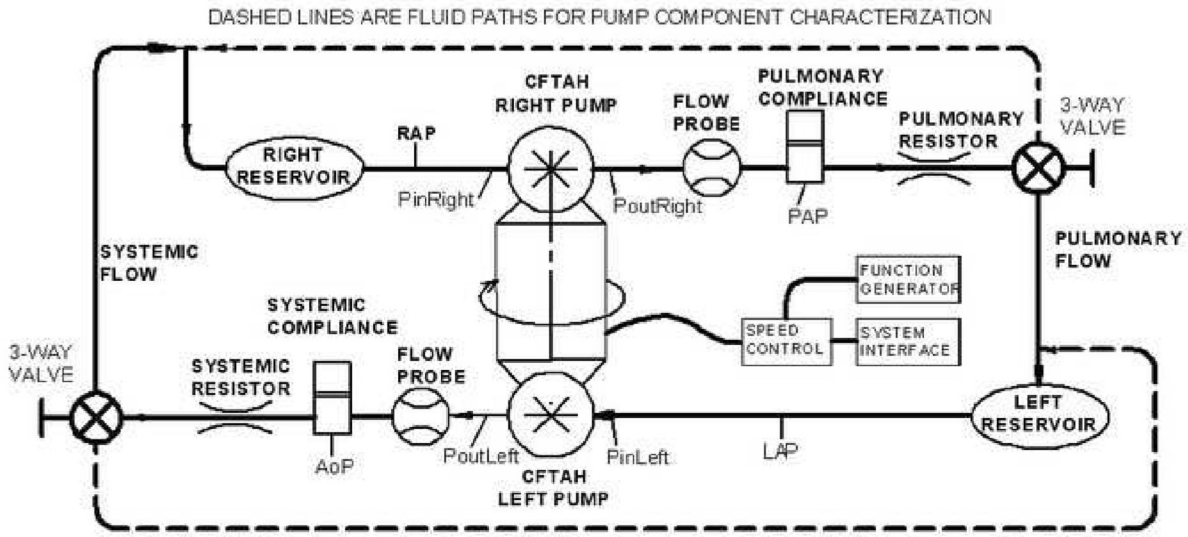

Figure 5.
Schematic drawing of TAH mock circulatory loop used in the *in vitro* tests.

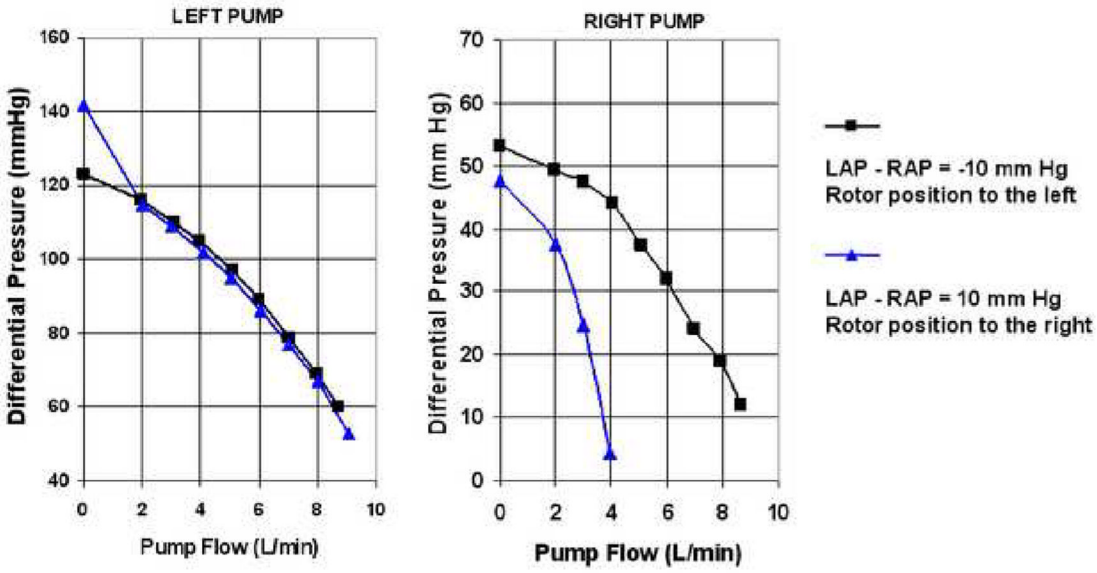

Figure 6.
Pump sensitivity to rotor axial position demonstrating self-regulating performance of left and right pumps.

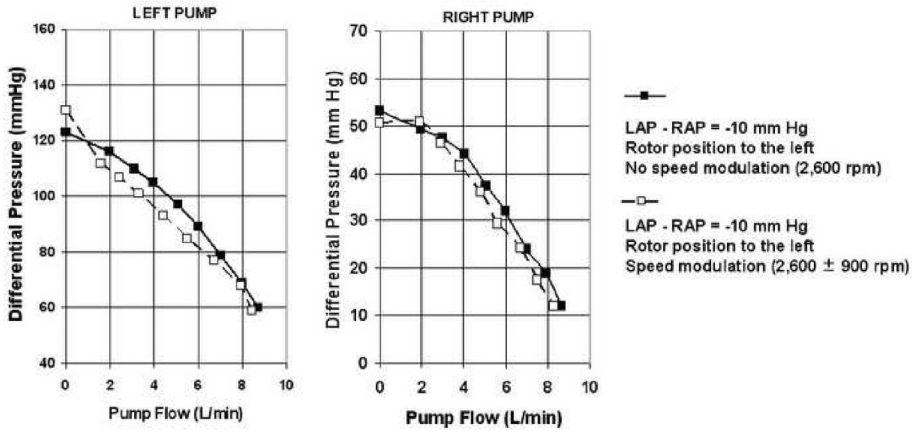

Figure 7.
Pump sensitivity to speed modulation with rotor position to the left.

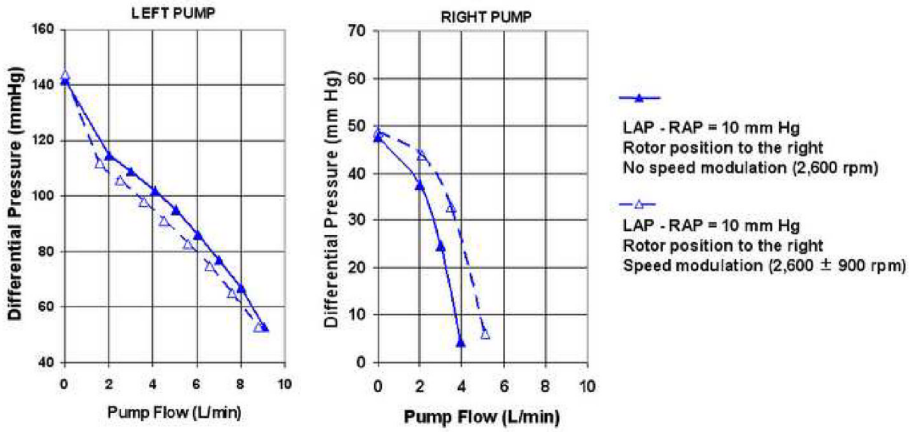

Figure 8.
Pump sensitivity to speed modulation with rotor position to the right.

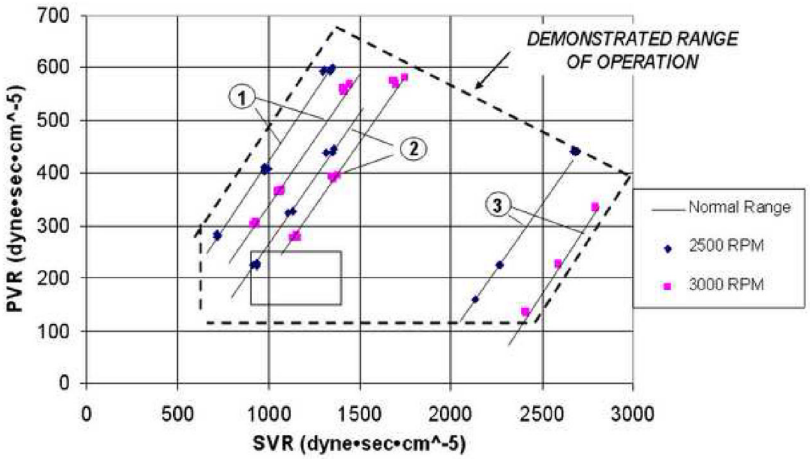

Figure 9.
Range of operation with extreme variation and mismatches of SVR and PVR.

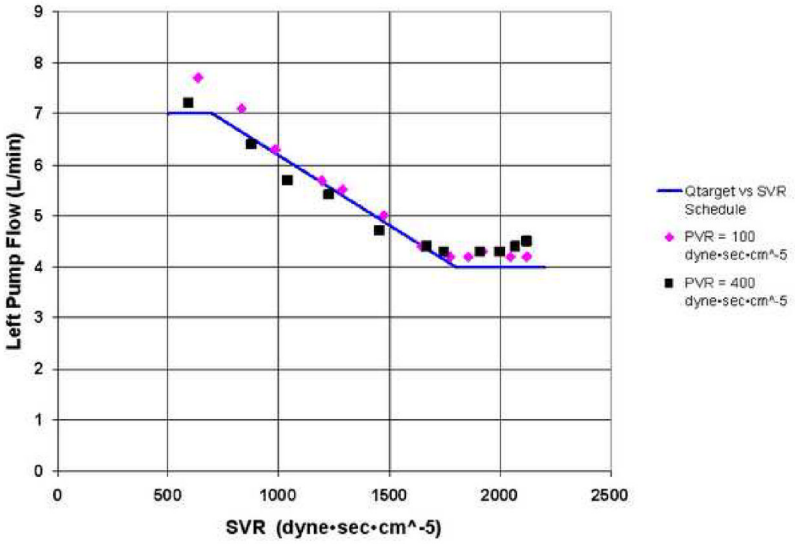

Figure 10.

Resulting measured left pump flow vs. measured SVR relationship for the given derived target CFTAH pump flow vs. calculated SVR relationship. Qtarget, target left pump flow; SVR, systemic vascular resistance; PVR, pulmonary vascular resistance.

Table 1

Atrial Pressure Differential Effects on Hydraulic Performance

Atrial pressure difference at pump inlets	Rotor position	Left hydraulic performance	Right hydraulic performance	Atrial pressure correction
RAP >> LAP (Figure 3a)	Left	No Change	↑↑↑ Increases	↑ LAP & ↓ RAP
LAP >> RAP (Figure 3b)	Right	No Change	↓↓↓ Decreases	↑ RAP & ↓ LAP

RAP, right atrial pressure; LAP, left atrial pressure.

Table 2

Comparison of Simplicity

Relative simplicity - Number of components

Feature	Pulsatile TAH	Two continuous-flow pumps	Proposed CFTAH
Motor windings	1	2	1
Rotating/sliding assemblies	1	2	1
Actuator assembly	1	0	0
Percutaneous cables or TETS	1	2	1
Motor controllers	1	2	1
Valves	4	0	0
Diaphragm/blood sack	2	0	0
Compliance chamber	1	0	0
Sensors	1	1	0
Total	**13**	**9**	**4**

TAH, total artificial heart; CFTAH, continuous-flow total artificial heart; TETS, transcutaneous energy transmission system.